arXiv:1910.02556v1 [eess.SY] 3 Oct 2019

Bio-inspired Learning of Sensorimotor Control for Locomotion

Tixian Wang, Amirhossein Taghvaei, and Prashant G. Mehta

***Abstract*— This paper presents a bio-inspired central pattern generator (CPG)-type architecture for *learning* optimal maneuvering control of periodic locomotory gaits. The architecture is presented here with the aid of a snake robot model problem involving planar locomotion of coupled rigid body systems. The maneuver involves clockwise or counterclockwise turning from a nominally straight path. The CPG circuit is realized as a coupled oscillator feedback particle filter. The collective dynamics of the filter are used to approximate a posterior distribution that is used to construct the optimal control input for maneuvering the robot. A Q-learning algorithm is applied to learn the approximate optimal control law. The issues surrounding the parametrization of the Q-function are discussed. The theoretical results are illustrated with numerics for a 5-link snake robot system.**

I. INTRODUCTION

The objective of this paper is to present a bio-inspired central pattern generator (CPG)-type sensori-motor control architecture to *learn* optimal maneuvers using *only* noisy sensor measurements and (online) reward. The dynamic and sensor models are assumed unknown. The architecture, depicted in Fig. 1, is presented here with the aid of a snake robot model problem involving planar locomotion of coupled rigid body systems.

The snake robot is modeled as n coupled rigid bodies. The configuration space of the system is split into two sets of variables: (i) the *shape* variable which describes the internal shape of the system; (ii) and the *group* variable which describes the global displacement and orientation of the system. The shape variables are actuated using motors at each joint to produce a nominal sinusoidal gait for the forward motion. The synthesis procedure for this gait is taken from [2], where it was shown to be optimal with respect to an energy cost function.

The learning problem is for the robot to learn to maneuver about this nominal gait. The particular maneuver is to turn the robot either clockwise or counter-clockwise, e.g., to avoid an obstacle in the environment. We assume noisy measurement of the shape variables and employ changes in friction coefficients, with respect to the surface, as control inputs.

The main complexity reduction technique is to model the nominal periodic motion of the (local) shape variable at the j-th joint in terms of a single (hidden) phase variable $\theta_j(t)$ for $j = 1, 2, \ldots, n-1$. The inspiration comes from neuroscience where phase reduction is a popular technique to obtain reduced order model of neuronal dynamics [4].

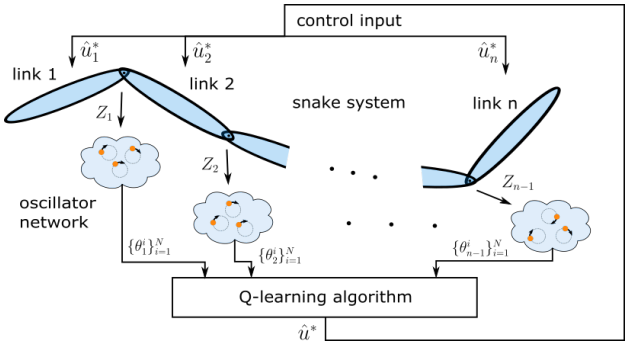

Fig. 1. The proposed architecture to learn a distributed feedback control law for turning the snake robot.

A coupled oscillator feedback particle filter (FPF) is used to approximate the posterior distribution of $\theta_j(t)$ given noisy measurements. The collective dynamics of the $(n-1)$ oscillator populations electrically encode the evolution of the mechanical shape of the robot. The filter requires knowledge of the observation model which is also learned in an online fashion through the use of a linear parameterization.

The filter outputs are aggregated into the second layer which seeks to learn the Q-function (or the Hamiltonian) based on an online access to the reward. A clever linear parametrization is used to enforce a distributed architecture for the policy. The parameters are learned by using a gradient descent algorithm to reduce the Bellman error [12], [5].

This overall control system can be viewed as a central pattern generator (CPG) which integrates sensory information to learn closed-loop optimal control policies for bio-locomotion. The framework presented here is based upon our prior research in [10] where phase reduction technique was introduced for a 2-link system and in [13] where the technique was extended to include learning for the 2-link system. The main contributions of this work over and above these prior publications are as follows:

1) The application involving the snake robot is new and more practically motivated than the simple 2-link model considered in [13].
2) The distributed coupled oscillator FPF is biologically motivated. Each of the FPF encodes only the local shape and can be extended to n-links and ultimately to a continuum rod type models. In contrast, the framework in our earlier papers parametrized the limit cycle by a single oscillator.
3) A procedure to learn the sensor model is presented. This

Financial support from the ONR MURI grant N00014-19-1-2373 and the ARO grant W911NF1810334 is gratefully acknowledged.

T. Wang, A. Taghvaei and P. G. Mehta are with the Coordinated Science Laboratory and the Department of Mechanical Science and Engineering at the University of Illinois at Urbana-Champaign (UIUC). tixianw2@illinois.edu; taghvae2@illinois.edu; mehtapg@illinois.edu

is in contrast to [10], [13], where the sensor model is assumed to be known.

4) The learning framework is numerically demonstrated in a simulation environment. The main innovation is the parametrization of the Q-function (or the Hamiltonian).

Taken together, the numerical results of this paper demonstrate an end-to-end architecture for sensori-motor control of bio-locomotion. These results are likely to spur comparative studies as well as theoretical investigations of learning in bio-locomotion.

The remainder of this paper is organized as follows: The snake system problem is formulated in Section II. The control problem solution is described in Section III. The numerical results of the snake system appear in Section IV.

II. Problem Formulation

A. Modeling

The model of snake robot, described next, closely follows [8]. Consider a system of n planar rigid links, connected by single degree of freedom joints as depicted in Fig. 2. The system is placed on a horizontal surface, subject to friction. The j-th joint is equipped with torque actuator (motor) with drive torque τ_j, linear torsional spring with coefficient κ_j, and viscous friction with coefficient ζ_j for $j = 1,\dots,n-1$. It is assumed that each link has uniformly distributed mass. For link j, m_j denotes its mass, l_j denotes its half length, and J_j denotes its moment of inertia about the center of mass.

The absolute orientation of j-th link, with respect to a global inertial frame, is denoted by $q_j \in [0, 2\pi]$, and the position of the center of mass is denoted by $r_{\text{CM}} \in \mathbb{R}^2$. As a result, $(q, r_{\text{CM}}) \in [0,2\pi]^n \times \mathbb{R}^2$, with $q := (q_1,\dots,q_n)$, represents the configuration of the n-link system.

The configuration is divided into two sets: (i) the shape variable; (ii) and the group variable. The shape variable, $x = (x_1,\dots,x_{n-1}) \in [0,2\pi]^{n-1}$, are the relative angle between the links, defined as $x_j = q_j - q_{j+1}$ for $j = 1,\dots,n-1$. The group variable $(\psi, r_{\text{CM}}) \in SE(2)$ comprises the global orientation of the system,

$$\psi := \frac{1}{n}\sum_{j=1}^{n} q_j \tag{1}$$

and the position of center of mass r_{CM}. The group variable is an element of the group of planar rigid body motions $SE(2)$.

An open loop periodic input is assumed for torque actuators,

$$\tau_j(t) = \tau_{0\,j}\sin(\omega_0 t + \beta_j), \quad \text{for } j = 1,\dots,n-1 \tag{2}$$

where ω_0 is frequency, $\tau_{0\,j}$ is the amplitude, and β_j is the phase. The particular form of the periodic input is not important. For the purpose of numerics, this input is chosen to induce a nominal gait, which leads to forward motion.

The friction force exerted at each link comprises of three component: A force component directed normal to the link, a force component directed tangent to the link, and a torque.

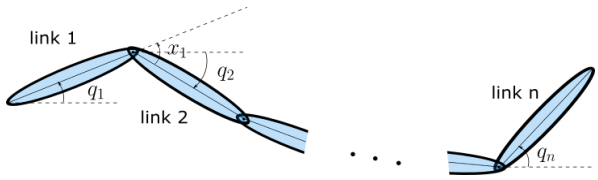

Fig. 2. Schematic of the n-link system for the snake robot.

The models for these components are,

$$\begin{aligned}\text{normal friction force} &= -c_{n,j} m_j v_j \cdot \hat{n}_j \\ \text{tangent friction force} &= -c_{t,j} m_j v_j \cdot \hat{t}_j \\ \text{friction torque} &= -c_{n,j} J_j \dot{q}_j\end{aligned}$$

where $\hat{n}_j$, $\hat{t}_j$ are the normal and tangent unit vectors to link j, v_j is the velocity of link j, and $c_{t,j}, c_{n,j}$ are the friction coefficients in the tangent and normal directions, respectively. For snake robot, these coefficients are different ($c_n \gg c_t$) which is believed be essential for forward locomotion [3].

For the snake robot model problem, the control input enters via change in friction coefficients as,

$$c_{n,j}(t) = \bar{c}_{n,j}(1 + u_j(t)), \quad \text{for } j = 1,\dots,n \tag{3}$$

where $\bar{c}_{n,j}$ is the nominal friction coefficient normal to link j, and $u_j(t)$ represents a small time-dependent perturbation due to control.

B. Dynamics

The dynamics of the system is given by a second order ode for the shape variable, and a first-order ode for the group variable:

$$\ddot{x}(t) = \tilde{F}_x(x(t), \dot{x}(t), \tau(t), u(t)), \tag{4}$$

$$\frac{\mathrm{d}}{\mathrm{d}t}\begin{bmatrix}\psi(t) \\ r_{\text{CM}}(t)\end{bmatrix} = \begin{bmatrix}\tilde{F}_\psi(x(t), \dot{x}(t), u(t)) \\ \tilde{F}_r(x(t), \dot{x}(t), u(t))\end{bmatrix} \tag{5}$$

The derivation of the dynamic equations and the explicit form of the functions $\tilde{F}_x$, $\tilde{F}_\psi$, and $\tilde{F}_r$ appears in Appendix A. In this paper, the explicit form of these functions are assumed to be unknown.

C. Observation process

The shape variable and its velocity $(x, \dot{x})$ are assumed not to be fully observed . To estimate $(x, \dot{x})$, each joint is equipped with a sensor that provides noisy measurements of the shape variable and its velocity. The model for the sensor at the j-th joint is

$$\mathrm{d}Z_j(t) = \tilde{h}_j(x_j(t), \dot{x}_j(t))\,\mathrm{d}t + \sigma_W\,\mathrm{d}W_j(t), \quad \text{for} j = 1,\dots,n-1 \tag{6}$$

where $W_j(t)$ is a standard Wiener process and σ_W is the standard deviation parameter. The explicit form of the function $\tilde{h}_j(\cdot)$ in the observation model is assumed to be unknown. However, it is assumed that $\tilde{h}_j(\cdot)$ is only a function of $(x_j, \dot{x}_j)$.

D. Optimal control problem

The control objective is to find a control input $u(t)$ that turns the robot, while the robot is moving forward with a nominal gait produced by the uncontrolled open-loop input torque $\tau(t)$ according to (2). The control objective is modeled as a discounted infinite-horizon optimal control problem:

$$\tilde{J}(x(0),\dot{x}(0)) = \min_{u(\cdot)} \mathsf{E}\left[\int_0^\infty e^{-\gamma t}\tilde{c}(x(t),\dot{x}(t),u(t))\,\mathrm{d}t\right] \quad (7)$$

subject to the dynamic constraints (4). Here, $\gamma > 0$ is the discount rate and the cost function

$$\tilde{c}(x,\dot{x},u) = \tilde{F}_\psi(x,\dot{x},u) + \frac{1}{2\varepsilon}\|u\|_2^2 \quad (8)$$

where $\tilde{F}_\psi(x,\dot{x},u) = \dot{\psi}$ is the rate of change of the global orientation ψ, $\|u\|_2^2 = \sum_{j=1}^n u_j^2$, and $\varepsilon > 0$ is the control penalty parameter. The minimum is over all control inputs $u(\cdot)$ adapted to the filtration $\mathscr{Z}_t := \sigma(Z(s); s \in [0,t])$ generated by the observation process.

The cost function is chosen so that, minimizing the cost leads to negative net change in the global orientation ψ, which corresponds to the clockwise rotation.

III. Solution Approach

Solving the optimal control problem (7) is challenging because:

1) The function $\tilde{F}_x$ in the dynamics model (4) for the $(n-1)$-dimensional shape variable x is assumed to be unknown. The model is highly nonlinear due to the details of the geometry and contact forces with the environment (see (32) in Appendix A).
2) The explicit form of the function $\tilde{F}_\psi$ that appears in the cost function (8) is assumed to be unknown.
3) The shape variable $(x,\dot{x})$ is not fully observed.
4) The explicit form of the observation functions $\tilde{h}_j(\cdot)$ in (6) are assumed to be unknown.

The following steps are used to overcome these challenges:

A. Step 1. Phase modeling

Consider the second-order differential equation (4) for the shape variable x under the open-loop periodic input $\tau(t)$ in (2). The following assumption is made concerning its solution:

Assumption A1 Under periodic forcing $\tau(t)$ as in (2), the solution $(x_j(t),\dot{x}_j(t))$ to (4) is an isolated asymptotically stable periodic orbit (limit cycle) with period $2\pi/\omega_0$ for $j = 1,\dots,n-1$ (see Figure 3).

Denote the set of points on the limit cycle of $(x_j(t),\dot{x}_j(t))$ as $\mathscr{P}_j \subset \mathbb{R}^2$. Each limit cycle solution is parameterized by a phase coordinate $\theta_j \in [0,2\pi)$ in the sense that there exists an invertible map $X_j^{LC} : [0,2\pi) \to \mathscr{P}_j$ such that $X_j^{LC}(\theta_j(t)) = (x_j(t),\dot{x}_j(t))$, where $\theta_j(t) = (\omega_0 t + \theta_j(0)) \bmod 2\pi$, for $j = 1,\dots,n-1$. The definition of the phase variable is extended locally in a small neighborhood of the limit cycle by using the notion of isochrons [4].

Let $\theta(t) := (\theta_1(t),\dots,\theta_{n-1}(t))$ denote the vector of all the phase variables, and $X^{LC}(\theta) := (X_1^{LC}(\theta_1),\dots,X_{n-1}^{LC}(\theta_{n-1}))$. In terms of $\theta(t)$, the first-order dynamics of the group variable in (5) is expressed as

$$\frac{\mathrm{d}}{\mathrm{d}t}\begin{bmatrix}\psi(t)\\ r_{\mathrm{CM}}(t)\end{bmatrix} = \begin{bmatrix}\tilde{F}_\psi(X^{LC}(\theta(t)),u(t))\\ \tilde{F}_r(X^{LC}(\theta(t)),u(t))\end{bmatrix} =: \begin{bmatrix}F_\psi(\theta(t),u(t))\\ F_r(\theta(t),u(t))\end{bmatrix} \quad (9)$$

and the observation model (6) is

$$\mathrm{d}Z_j(t) = h_j(\theta_j(t))\,\mathrm{d}t + \sigma_W\,\mathrm{d}W_j(t), \quad \text{for } j = 1,\dots,n-1 \quad (10)$$

where $h_j(\theta_j) := \tilde{h}_j(X_j^{LC}(\theta_j))$.

The optimal control problem (7) in terms of the phase vector is given by

$$J(\theta(0)) = \min_{u(\cdot)} \mathsf{E}\left[\int_0^\infty e^{-\gamma t}c(\theta(t),u(t))\,\mathrm{d}t\right] \quad (11)$$

where $c(\theta,u) = F_\psi(\theta,u) + \frac{1}{2\varepsilon}\|u\|_2^2$ and the minimum is over all control inputs $u(\cdot)$ adapted to the filtration $\mathscr{Z}_t$.

The new problem is described by a single phase vector θ instead of coupled shape variables x and $\dot{x}$. With $u(t) \equiv 0$, the dynamics is described by the oscillator model $\theta_j(t) = (\omega_0 t + \theta_j(0)) \bmod 2\pi$ for $j = 1,\dots,n-1$. Now, in the presence of (small) control input, the dynamics need to be augmented by an additional term $\varepsilon g(\theta,u)$ due to control:

$$\mathrm{d}\theta(t) = (\omega_0 1_{n-1} + \varepsilon g(\theta(t),u(t)))\,\mathrm{d}t \quad (12)$$

where $1_{n-1} = [1,\dots,1]^T \in \mathbb{R}^{n-1}$.

B. Step 2. Learning observation model

The explicit form of the function $h_j(\cdot)$ in the observation model (10) is not known. It is approximated using a linear combination of the Fourier basis functions:

$$h_j(\theta_j) \approx h_j(\theta_j; r_j) := r_j^T \phi_h(\theta_j), \quad \text{for } j = 1,\dots,n-1 \quad (13)$$

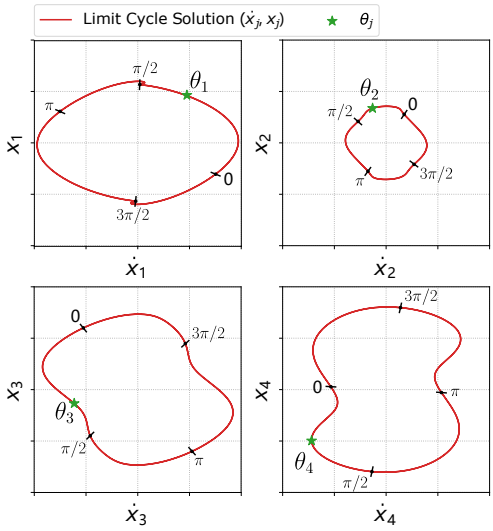

Fig. 3. The limit cycle solution for the shape variable $(x(t),\dot{x}(t))$ under the periodic torque input (2), for a 5-link system. Each limit cycle is parametrized with a phase variable $\theta_j \in [0,2\pi]$.

where ϕ_h is a vector of M_h Fourier basis functions (e.g $\phi_h(\vartheta) = (\sin(\vartheta), \cos(\vartheta))$), and $r_j \in \mathbb{R}^{M_h}$ is a vector of M_h weights. The weights are initialized at zero and updated in an online fashion according to

$$\mathrm{d}r_j(t) = \alpha_h(t) \left[\mathrm{d}Z_j(t) - \hat{h}_j(t)\,\mathrm{d}t \right] \mathsf{E}[\phi_h(\theta_j(t)) | \mathscr{Z}_t] \tag{14}$$

where $\alpha_h(t)$ is the learning rate, and $\hat{h}_j(t) := \mathsf{E}[h_j(\theta_j(t), r_j(t)) | \mathscr{Z}_t]$. In numerical implementation, the conditional expectations are approximated using the feedback particle filter, described next.

C. Step 3. Feedback particle filter (FPF)

The feedback particle filter algorithm is used to obtain the posterior distribution of the phase vector $\theta(t)$, governed by dynamics (12), given the noisy observations (10). The filter comprises N stochastic processes $\{\theta^i(t) : 1 \le i \le N\}$, where $\theta^i(t) \in [0, 2\pi]^{n-1}$ is the state of the i-th particle (oscillator) at time t. The particles evolve according to

$$\begin{aligned} \mathrm{d}\theta^i(t) &= \omega^i 1_{n-1}\,\mathrm{d}t + \varepsilon g(\theta^i(t), u(t))\,\mathrm{d}t \\ &+ \sum_{j=1}^{n-1} \frac{\mathsf{K}_j(\theta^i(t), t)}{\sigma_W^2} \circ \left(\mathrm{d}Z_j(t) - \frac{h_j(\theta_j^i(t), r_j(t)) + \hat{h}_j(t)}{2}\,\mathrm{d}t \right) \end{aligned} \tag{15}$$

where $\omega^i \sim \mathrm{Unif}([\omega_0 - \delta, \omega_0 + \delta]^{n-1})$ is the frequency of the i-th oscillator, $\hat{h}_j(t) := \mathsf{E}[h_j(\theta_j(t), r_j(t)) | \mathscr{Z}_t]$, and the notation $\circ$ denotes Stratonovich integration. In numerical implementation $\hat{h}_j(t) \approx \frac{1}{N} \sum_{i=1}^N h_j(\theta_j^i(t), r_j(t))$.

The algorithm involves $n-1$ gain functions $\mathsf{K}_j(\theta, t)$ for $j = 1, \ldots, n-1$, where the j-th gain function corresponds to the j-th observation signal. Each gain function is a $(n-1)$-dimensional vector expressed as $\mathsf{K}_j(\theta, t) = (\mathsf{K}_{j,1}(\theta, t), \ldots, \mathsf{K}_{j,n-1}(\theta, t)) \in \mathbb{R}^{n-1}$. The gain function is the solution of a certain partial differential equation. In practice, the gain function is numerically approximated using the Galerkin algorithm. The details of the Galerkin algorithm appears in [11].

Given the particles, the conditional expectation $\mathsf{E}[f(\theta(t)) | \mathscr{Z}_t]$ of a given function $f(\cdot)$ is approximated as $\frac{1}{N} \sum_{i=1}^N f(\theta^i(t))$.

Remark 1: There are two manners in which control input $u(t)$ affects the dynamics of the filter state $\theta^i(t)$:

1) The $O(\varepsilon)$ term $\varepsilon g(\cdot, u(t))$ which models the effect of dynamics;
2) The FPF update term which models the effect of sensor measurements. This is because the control input $u(t)$ affects the state $(x(t), \dot{x}(t))$ (see (4)) which in turn affects the sensor measurements $Z(t)$ (see (6)).

D. Step 4. Q-learning

With the constructed FPF, we can now express the partially observed optimal control problem (11) as a fully observed optimal control problem in terms of oscillator states $\theta^{(N)}(t) = (\theta^1(t), \ldots, \theta^N(t))$ according to

$$J^{(N)}(\theta^{(N)}(0)) = \min_{u(\cdot)} \mathsf{E} \left[\int_0^\infty e^{-\gamma t} c^{(N)}(\theta^{(N)}(t), u(t))\,\mathrm{d}t \right] \tag{16}$$

subject to (14)-(15), where the cost $c^{(N)}(\theta^{(N)}, u) := \frac{1}{N} \sum_{i=1}^N c(\theta^i, u)$ and the minimization is over all control laws adapted to the filtration $\mathscr{Z}_t := \{\theta^i(s);\ s \le t, 1 \le i \le N\}$. The problem is now fully observed because the states of oscillators $\theta^{(N)}(t)$ are known. This approach closely follows [6].

The analogue of the Q-function for continuous-time systems is the Hamiltonian function:

$$H^{(N)}(\theta^{(N)}, u) = c^{(N)}(\theta^{(N)}, u) + \mathscr{D}_u J^{(N)}(\theta^{(N)}) \tag{17}$$

where $\mathscr{D}_u$ is the generator for (15) defined such that $\frac{\mathrm{d}}{\mathrm{d}t} \mathsf{E}[J^{(N)}(\theta^{(N)}(t))] = \mathscr{D}_u J^{(N)}(\theta^{(N)}(t))$.

The dynamic programming principle for the discounted problem implies:

$$\min_u\ H^{(N)}(\theta^{(N)}, u) = \gamma J^{(N)}(\theta^{(N)}) \tag{18}$$

Substituting this into the definition of the Hamiltonian (17) yields the fixed-point equation:

$$\mathscr{D}_u\ \underline{\mathrm{H}}^{(N)}(\theta^{(N)}) = -\gamma (c^{(N)}(\theta^{(N)}, u) - H^{(N)}(\theta^{(N)}, u)) \tag{19}$$

where $\underline{\mathrm{H}}^{(N)}(\theta^{(N)}) := \min_u\ H^{(N)}(\theta^{(N)}, u)$. This is equivalent to the fixed-point equation that appears in the Q-learning algorithm in discrete-time setting.

Linear function approximation: The Hamiltonian function is approximated as the linear combination of M real-valued basis functions $\{\phi_m(\theta, u)\}_{m=1}^M$ as follows:

$$\hat{H}^{(N)}(\theta^{(N)}, u; w) = \frac{1}{N} \sum_{i=1}^N w^T \phi(\theta^i, u) \tag{20}$$

where $w \in \mathbb{R}^M$ is a vector of weights and $\phi = (\phi_1, \ldots, \phi_M)^T$ is a vector of basis functions. Thus, the infinite-dimensional problem of learning the Hamiltonian function is reduced to the problem of learning the M-dimensional weight vector w.

We define the point-wise Bellman error as follows:

$$\begin{aligned} \mathscr{E}(\theta^{(N)}, u; w) :=& \mathscr{D}_u \hat{\underline{\mathrm{H}}}^{(N)}(\theta^{(N)}; w) \\ &+ \gamma (c^{(N)}(\theta^{(N)}, u) - \hat{H}^{(N)}(\theta^{(N)}, u; w)) \end{aligned} \tag{21}$$

where $\hat{\underline{\mathrm{H}}}^{(N)}(\theta^{(N)}; w) := \min_u\ \hat{H}^{(N)}(\theta^{(N)}, u; w)$.

Then a gradient descent algorithm to learn the weights is:

$$\frac{\mathrm{d}}{\mathrm{d}t} w(t) = -\frac{1}{2} \alpha(t) \nabla_w \mathscr{E}^2(\theta^{(N)}(t), u(t); w(t)) \tag{22}$$

where $\alpha(t)$ is the learning rate and $u(t)$ is chosen to explore the state-action space. For the convergence analysis of the Q-learning algorithm, see [9], [7].

Given a learned weight vector w^*, the learned optimal control policy is given by:

$$\hat{u}^*(\theta^{(N)}; w^*) = \arg\min_v\ \hat{H}^{(N)}(\theta^{(N)}, v; w^*) \tag{23}$$

E. Information structure

In order to implement the FPF algorithm (15), it is necessary to know the model for $g(\theta,u)$. The function $g(\theta,u)$ represents the effect of the control input on the limit cycle. However, it is numerically observed that the control input has negligible effect on the limit cycle solution. Thus, in the simulation results presented next, the term $\varepsilon g(\theta^i(t),u(t))$ is ignored.

In the Q-learning algorithm, the generator $\mathscr{D}_u$ is approximated numerically as

$$\mathscr{D}_u\hat{\underline{\mathrm{H}}}^{(N)}(\theta^{(N)}(t)) \approx \frac{\hat{\underline{\mathrm{H}}}^{(N)}(\theta^{(N)}(t+\Delta t)) - \hat{\underline{\mathrm{H}}}^{(N)}(\theta^{(N)}(t))}{\Delta t}$$

where Δt is the discrete time step-size and $\{\theta^i(t)\}_{i=1}^N$ is the state of the oscillators at time t.

The function $F_\psi(\theta(t),u(t))$ that appears in the cost function is numerically approximated as

$$F_\psi(\theta(t),u(t)) = \dot{\psi}(t) \approx \frac{\psi(t+\Delta t)-\psi(t)}{\Delta t}$$

where Δt is the discrete time step-size in the numerical algorithm and $\psi(t)$ is available through a (black-box) simulator, that simulates the dynamics (4) and (5).

F. Distributed aspect of the architecture

The FPF algorithm (15) is simplified to $n-1$ independent filters as follows. By ignoring the $\varepsilon g(\theta,u)$ term in (12), the evolution of the each component $\theta_j \in [0,2\pi]$ of the $n-1$ dimensional phase variable $\theta \in [0,2\pi]^{n-1}$ becomes independent of each other. Moreover, the observation functions $h_j(\cdot)$ for $j=1,\dots,n-1$ in the sensor model (10) are independent of each other, in the sense that $h_j(\cdot)$ is a function of only θ_j. Therefore, the posterior distribution of the phase variable θ is the product of $n-1$ independent distributions for θ_j. With independent posterior distribution, the j-th gain function $\mathsf{K}_j(\theta,t) \in \mathbb{R}^{n-1}$ in the FPF algorithm (15) takes the form $\mathsf{K}_j(\theta,t) = (0,\dots,0,\mathsf{K}_{j,j}(\theta_j,t),0,\dots,0) \in \mathbb{R}^{n-1}$. As a result, the FPF algorithm is decomposed to $n-1$ independent filters. The evolution of particles $\{\theta_j^i(t)\}_{i=1}^N$ for the j-th filter is

$$\begin{aligned}\mathrm{d}\theta_j^i(t) &= \omega^i\,\mathrm{d}t \\ &+ \frac{\mathsf{K}_{j,j}(\theta_j^i(t),t)}{\sigma_W^2} \circ \left(\mathrm{d}Z_j(t) - \frac{h_j(\theta_j^i(t),r_j(t)) + \hat{h}_j(t)}{2}\,\mathrm{d}t\right)\end{aligned} \tag{24}$$

Therefore, the FPF algorithm for each joint is simulated independently from the other FPFs for other joints, in a distributed manner as shown in Figure 1.

The learned control input is also designed to take distributed structure, in the sense that the control input to each link depends only on the phase variable of its adjacent joints. The distributed structure is enforced by a careful selection of basis functions for the Hamiltonian in (20). The selected basis functions consist of three groups:

$$\begin{aligned}&\text{group 1:} && \{\Phi(\theta_j)\}_{j=1}^{n-1} \\ &\text{group 2:} && \{u_j\Phi(\theta_j), u_{j+1}\Phi(\theta_j)\}_{j=1}^{n-1} \\ &\text{group 3:} && \{\frac{1}{2}u_j^2\}_{j=1}^{n}\end{aligned} \tag{25}$$

where $\Phi(\vartheta) = (\Phi_1(\vartheta),\dots,\Phi_{M_F}(\vartheta))$ is a vector of selected Fourier basis functions (e.g $\Phi(\vartheta) = (\sin(\vartheta),\cos(\vartheta))$). With this particular form of basis functions, the j-th component of the learned control input (23) takes the following form:

$$\hat{u}_j^*(\theta^{(N)},w^*) = \frac{1}{N}\sum_{i=1}^{N}\sum_{m=1}^{M_F} a_{j,m}\Phi_m(\theta_j^i) + b_{j,m}\Phi_m(\theta_{j-1}^i) \tag{26}$$

where the constants $a_{j,m}$ and $b_{j,m}$ depend on the value of optimal weight vector w^*, and the convention $b_{1,m} = a_{n,m} = 0$ is assumed, for $m = 1,\dots,M_F$. According to the formula (26), the control input to j-th link, only depends on the phase of the adjacent joints θ_j and θ_{j-1}. The overall numerical procedure is summarized in Algorithm 1.

Algorithm 1 The proposed numerical algorithm

Input: A simulator for (4)-(5)-(6).
Output: Optimal control policy $\hat{u}^*(\theta^{(N)};w)$.

Initialize weight vector w_0
Initialize particles $\left\{\{\theta_j^i(0)\}_{i=1}^N\right\}_{j=1}^{n-1} \sim \mathrm{Unif}([0,2\pi])$;
for the $k=1$ to $n_T\frac{2\pi}{\omega_0\Delta t}$ **do**
  Choose control input $u(k)$ according to (27);
  Input $u(k)$ to simulator and output $Z(k),\psi(k)$;
  for the $j=1$ to $n-1$ **do**
    Compute $\hat{h}_j(k) = \frac{1}{N}\sum_{i=1}^N h_j(\theta_j^i(k),r_j(k))$ and $\Delta Z_j(k) = Z_j(k+1) - Z_j(k)$
    Update the weights for observation model

$$r_j(k+1) = r_j(k) + \alpha_h\left[\Delta Z_j(k) - \hat{h}_j(k)\Delta t\right]\frac{1}{N}\sum_{i=1}^N \phi_h(\theta_j(k)^i)$$

    Update the particles

$$\begin{aligned}\theta_j^i(k+1) &= \theta_j^i(k) + \omega^i\Delta t \\ &+ \frac{\mathsf{K}_{j,j}(\theta_j^i(k),k)}{\sigma_W^2}(\Delta Z_j(k) - \frac{h_j(\theta_j^i(k),r_j(k)) + \hat{h}_j(k)}{2}\Delta t)\end{aligned}$$

  end for
  Compute cost $c(k) = \frac{\psi(k+1)-\psi(k)}{\Delta t} + \frac{1}{2\varepsilon}\|u(k)\|_2^2$
  Compute Bellman error

$$\mathscr{E}(k) = \mathscr{D}_u\hat{\underline{\mathrm{H}}}^{(N)}(k) + \gamma(c(k) - \hat{H}^{(N)}(\theta^{(N)}(k),u(k);w(k)))$$

  Update weight $w(k+1) = w(k) - \Delta t\alpha\mathscr{E}(k)\nabla_w\mathscr{E}(k)$
end for
Output the learned control $\hat{u}^*(\theta^{(N)};w(k))$ from (23).

IV. Numerics

The following numerical results are for the snake robot with $n=5$ links. The numerical results are based on Algorithm 1. The simulation parameters are tabulated in Table I.

TABLE I

PARAMETERS FOR NUMERICAL SIMULATION

Parameter	Description	Numerical value
	Sensor & FPF	
Δt	Discrete time step-size	0.02
σ_W	Noise process std. dev.	0.1
N	Number of particles	100
δ	Heterogeneous parameter	0.05
	Q-learning	
n_e	number of episodes	200
n_T	number of periods in each episode	10
ε	Control penalty parameter	10.0
γ	Discount rate	0.50
α	Learning gain for Q-learning	0.01
α_h	Learning gain for observation model	0.01

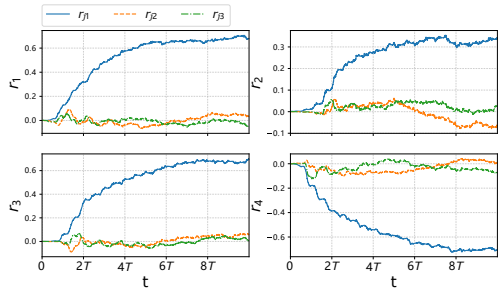

Fig. 4. The time-trace of the weights for learning the observation model according to (14).

A. Learning the observation model and FPF

The observation signal $y_j(t) := (Z_j(t+\Delta t) - Z_j(t))/\Delta t$, for $j = 1,2,3,4$ is depicted in Figure 5. The signal is generated according to (6), with observation function taken as $\tilde{h}_j(x_j, \dot{x}_j) = x_j$. The noise strength $\sigma_w = 0.1$.

The Fourier basis functions used to approximate the observation function according to (13) are

$$\phi_h(\vartheta) = (\sin(\vartheta), \sin(2\vartheta), \cos(2\vartheta))$$

Including the $\cos(\vartheta)$ in the basis functions is redundant because of the degeneracy in defining the phase.

The gradient descent algorithm (14), to learn the weights r_j, and the FPF algorithm (24), for the j-th joint are simulated, for $j = 1,2,3,4$. The time-trace of the weights $r_j(t)$, and the trajectory of particles $\theta_j^i(t)$, are depicted in Figure 4 and 6 respectively.

The performance of the observation model learning algorithm and the FPF algorithm is observed in Figure 5. The figure includes three signals: (i) The noisy measurements $y_j(t)$; (ii) the value $\tilde{h}_j(x_j(t), \dot{x}_j(t)) = x_j(t)$; (iii) and the approximation $\hat{h}_j(t) = \frac{1}{N}\sum_{i=1}^N h_j(\theta_j^i(t), r_j(t))$, which involve the learned wights $r_j(t)$ and the particles $\{\theta_j^i(t)\}_{i=1}^N$. It is observed that the approximation $\hat{h}_j(t)$ converges to the exact value $h_j(x_j(t), \dot{x}_j(t))$, as the learning for the weights converge and particles become synchronized.

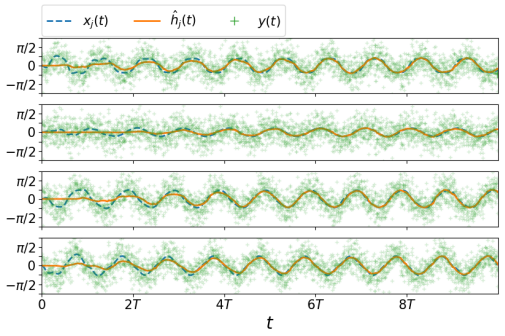

Fig. 5. The figure contains three signals: (i) $y_j(t)$: the noisy observation signal from the observation model (6) where $y(t) = (Z(t+\Delta t) - Z(t))/\Delta t$; (ii) The exact observation signal $\tilde{h}_j(x_j(t), \dot{x}_j(t)) = x_j(t)$; (iii) and the approximation $\hat{h}_j(t) = N^{-1}\sum_{i=1}^N h_j(\theta_j^i(t), r_j(t))$.

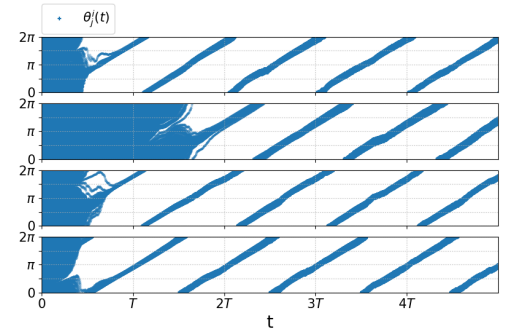

Fig. 6. Time trace of $N = 100$ particles for the four independent FPF algorithm (24). The empirical distribution of the particles for the j-th FPF approximates the posterior distribution of the phase variable corresponds to the j-th joint of the 5-link system.

B. Q-learning

The Q-learning algorithm is simulated for 200 episodes. Each episode starts with random initialization of the state, and continues for $n_T = 10$ periods.

The basis function used to approximate the Hamiltonian in (20) are chosen according to (25) with $\Phi(\vartheta) = (\cos(\vartheta), \sin(\vartheta), \cos(2\vartheta), \sin(2\vartheta))$.

The weights for the $\frac{1}{2}u_j^2$ basis function are initialized randomly with uniform distribution Unif$([0.09, 0.11])$. The rest of the weights are initialized according to Unif$([-0.1, 0.1])$

For the purpose of exploration, the control input $u(t)$ to be used in (22) is chosen as a combination of sinusoidal functions with irrational frequencies as follows:

$$u_j(t) = A\sin(\sqrt{2}\omega_0 t + \frac{j\pi}{5}) + A\sin(\pi\omega_0 t + \frac{j\pi}{5}) \qquad (27)$$

for $j = 1, \ldots, 5$ where $A = 0.5$. The rationale for choosing such control input is to explore the state-action space, which is essential for convergence of the Q-learning [1].

The L^2-norm of the point-wise Bellman error (21), averaged over the j-th episode, is defined according to

$$e_j := \frac{1}{n_T T}\int_{(j-1)n_T T}^{jn_T T} \left|\mathscr{E}(\theta^{(N)}(t), u(t); w(t))\right|^2 \mathrm{d}t \qquad (28)$$

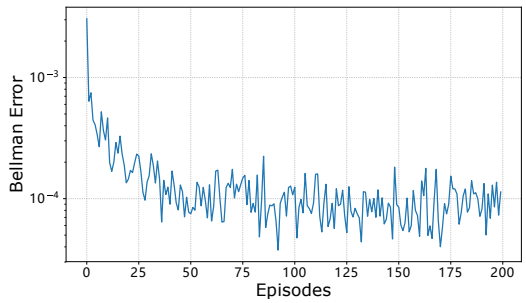

Fig. 7. Summary of the Q-learning algorithm result: Average Bellman error defined in (28) versus episode number.

The average Bellman error e_j as a function of episode is depicted in Figure 7. The decrease in the Bellman error implies that the algorithm is able to learn the Hamiltonian function that solves the approximate dynamic programming fixed-point equation (19).

Figure 8(a) depicts the learned control input $\hat{u}^*(\theta^{(N)}(t), w^*)$ evaluated according to (26) . Figure 8(b) depicts the resulting global displacement $r_{\text{CM}}(t)$ and the global orientation $\psi(t)$, driven with the learned control input. It is observed that the learned control input induces net change in the global orientation and turn the snake robot clockwise.

V. Conclusions and Future Work

A bio-inspired framework for learning a sensorimotor control of locomotion is introduced and illustrated with a planar coupled rigid body model of a snake robot. The framework does not require knowledge of the explicit form of the dynamics and the observation models.

Although the filtering and control are implemented in a distributed manner, the Q-learning algorithm is centralized. A possible direction of future work is to implement the learning in a distributed way, so that the overall architecture becomes fully distributed. Another direction for future work is to extend the current framework to continuum rod type of models, motivated by applications in soft-robotics.

Appendix

A. Derivation of the dynamic model

The dynamic equations are derived from Lagrangian mechanics approach. The Lagrangian $L = E(q,\dot{q}) - V(q)$ is the difference between kinetic energy $E(q,\dot{q})$ and potential energy $V(q)$, given by:

$$E(q,\dot{q}) = \frac{1}{2} m \dot{r}_{\text{CM}}^2 + \frac{1}{2} \dot{q}^T I_{(q)} \dot{q} \ , \quad V(q) = \sum_{j=1}^{n-1} \frac{1}{2} \kappa_j (q_j - q_{j+1})^2$$

where $m = \sum_{i=j}^{n} m_j$ is the total mass of the system, and $I_{(q)}$ is the inertia matrix. The Euler-Lagrange equation is,

$$\frac{\mathrm{d}}{\mathrm{d}t}\left(\frac{\partial L}{\partial \dot{q}}\right) - \frac{\partial L}{\partial q} = f^{\text{gen}} \tag{29}$$

TABLE II

Model Parameters for the n-link system

Parameter	Description
m_j	Mass of link j
J_j	Moment of inertia of link j
$2l_j$	Length of link j
$c_{t,j}$	friction coefficient tangent to link j
$c_{n,j}$	friction coefficient normal to link j
κ_j	Torsional spring coefficient at joint j
ζ_j	Viscous friction coefficient at joint j
τ_j	Input torque amplitude at joint j
ω_0	Input torque frequency
σ_w	Noise process std. dev.
ε	Control penalty parameter

Numerical values

$m_j = 1.0, \quad J_j = 1/3, \quad l_j = 1.0, \quad c_{t,j} = 0.1, \quad c_{n,j} = 0.5$

$\kappa_j = 3.0, \quad \zeta_j = 0.1$ for $j = 1,2,3,4$

$\tau_0 = [2.0, 1.1, 1.0, 2.0], \quad \omega_0 = 1.0, \quad \sigma_w^2 = 0.1, \quad \varepsilon = 10.0$

where $f^{\text{gen}} \in \mathbb{R}^{n+2}$ are the generalized forces. Generalized forces are defined by $\delta W = \delta q f^{\text{gen}}$ where δW is the virtual work done by nonconservative forces, under infinitesimal variation δq. Nonconservative forces include actuator torques, viscous friction at each joint, and friction force with surface.

Considering generalized forces, the equations of motion are succinctly expressed as,

$$\begin{aligned} I_{(q)}\ddot{q} + C_{(q)}\dot{q}^2 + \tilde{\kappa} q &= D^T \tau - \tilde{\zeta}\dot{q} - \mathsf{R}_{qq}\dot{q} - \mathsf{R}_{qr}\dot{r}_{\text{CM}} \\ \frac{\mathrm{d}}{\mathrm{d}t}(m\dot{r}_{\text{CM}}) &= -\mathsf{R}_{rr}\dot{r}_{\text{CM}} - \mathsf{R}_{qr}^T \dot{q} \end{aligned} \tag{30}$$

where $\tau = [\tau_1, \ldots, \tau_{n-1}]$ are the actuator torques, $\tilde{\kappa}$ is the stiffness matrix, and $\tilde{\zeta}$ is the friction coefficient matrix. The terms involving $\mathsf{R}_{qq}, \mathsf{R}_{qr}, \mathsf{R}_{rr}$ arise due to friction with the surface. The matrix $D \in \mathbb{R}^{n-1 \times n}$ is the difference operator. These parameters are tabulated in Table III. A detailed derivation of the equations of motion appears in [8].

Shape dynamics: The coordinate transformation $(x, \psi) \leftrightarrow q$ is given by

$$\begin{bmatrix} x \\ \psi \end{bmatrix} = \begin{bmatrix} D \\ \frac{1}{n} e^T \end{bmatrix} q \Rightarrow q = \begin{bmatrix} D^+ & e \end{bmatrix} \begin{bmatrix} x \\ \psi \end{bmatrix} \tag{31}$$

where $e = [1, \ldots, 1]^T \in \mathbb{R}^n$, and $D^+ = D^T (DD^T)^{-1}$. Then the dynamic equation for the shape variable x is,

$$\begin{aligned} \ddot{x} &= (D I_{(x)}^{-1} D^T)(\tau - \kappa x - \zeta \dot{x}) \\ &\quad + D I_{(x)}^{-1} (-C_{(q)}\dot{q}^2 - \mathsf{R}_{qq} D^+ \dot{x} - \mathsf{R}_{qq} e \dot{\psi} - \mathsf{R}_{qv} v) \end{aligned} \tag{32}$$

where $I_{(x)} := I_{(q(x))}$. This is the explicit form of the second order ode in (4).

Group dynamics: Define the total angular momentum $\mu = e^T I_{(q)} \dot{q}$, and the group velocity $v = R(\psi)^T \dot{r}_{\text{CM}}$ where $R(\psi) = \begin{bmatrix} \cos(\psi) & -\sin(\psi) \\ \sin(\psi) & \cos(\psi) \end{bmatrix}$ is the rotation matrix. The dynamics

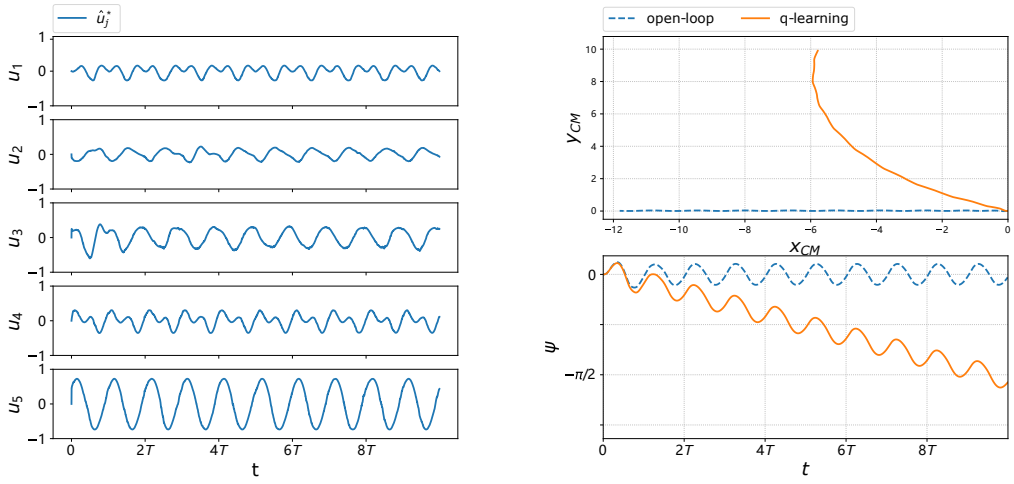

(a) (b)

Fig. 8. Summary of control results: (a) The learned control input (26) from the Q-learning algorithm; (b) Time trace of the global displacement $r_{\text{CM}} = (x_{\text{CM}}, y_{\text{CM}})$ and the global orientation ψ in open-loop manner ($u(t) = 0$), and using the learned control input.

TABLE III

AUXILIARY PARAMETERS FOR THE N-LINK SYSTEM

$$M = \text{diag}(m_j), \quad J = \text{diag}(J_j), \quad L = \text{diag}(l_j),$$
$$C_n = \text{diag}(c_{n,j}), \quad C_t = \text{diag}(c_{t,j})$$
$$[D]_{n-1\times n} \;\; s.t \;\; [Dx]_j = x_j - x_{j+1}, \quad [A]_{n-1\times n} \;\; s.t \;\; [Ax]_j = x_j + x_{j+1}$$
$$D^+ = D^T(DD^T)^{-1} \quad e = [1,\ldots,1]^T$$
$$\kappa = \text{diag}(\kappa_j), \quad \zeta = \text{diag}(\zeta_j), \quad \tilde{\kappa} = D^T\kappa D, \quad \tilde{\zeta} = D^T\zeta D$$
$$H = LA^T(DM^{-1}D^T)^{-1}AL, \quad B = M^{-1}D^T(DM^{-1}D^T)^{-1}AL$$

$$c_q = \cos(q_j), \quad s_q = \sin(q_j)$$
$$[I_{(q)}]_{ij} = H_{ij}\cos(q_i - q_j) + J_{ij} \quad [C_{(q)}]_{ij} = H_{ij}\sin(q_i - q_j)$$

$$[B_s]_{ij} = B_{ij}\sin(q_i - q_j) \quad [B_c]_{ij} = B_{ij}\cos(q_i - q_j)$$
$$\mathsf{R}_{qq} = B_s^T M C_t B_s + B_c^T M C_n B_c + C_n J$$
$$\mathsf{R}_{qv_1} = B_s^T M C_t c_{q-\psi} - B_c^T M C_n s_{q-\psi}$$
$$\mathsf{R}_{qv_2} = B_s^T M C_t s_{q-\psi} + B_c^T M C_n c_{q-\psi}$$
$$\mathsf{R}_{vv} = c_{q-\psi}^T M C_t c_{q-\psi} + s_{q-\psi}^T M C_n s_{q-\psi}$$
$$\mathsf{R}_{v_2v_2} = s_{q-\psi}^T M C_t s_{q-\psi} + c_{q-\psi}^T M C_n c_{q-\psi}$$
$$\mathsf{R}_{v_1v_2} = s_{q-\psi}^T M (C_t - C_n) c_{q-\psi}$$
$$\mathsf{R}_{qr} = \mathsf{R}_{qv} R^T(\psi), \quad \mathsf{R}_{rr} = R(\psi)\mathsf{R}_{vv}R^T(\psi)$$

for these two variables are

$$\begin{aligned} \frac{\mathrm{d}\mu}{\mathrm{d}t} &= -e^T\mathsf{R}_{qq}e\dot{\psi} - e^T\mathsf{R}_{qv}v - e^T\mathsf{R}_{qq}D^+\dot{x} \\ \frac{\mathrm{d}mv}{\mathrm{d}t} &= -m\begin{bmatrix} 0 & -\dot{\psi} \\ \dot{\psi} & 0 \end{bmatrix} v - \mathsf{R}_{vv}v - \mathsf{R}_{vq}e\dot{\psi} - \mathsf{R}_{vq}D^+\dot{x} \end{aligned} \tag{33}$$

Assuming the inertial terms are negligible, a first order ode is obtain for the evolution of the group variables (r_{CM}, ψ):

$$\frac{\mathrm{d}}{\mathrm{d}t}\begin{bmatrix} \psi \\ R(\psi)^T r_{\text{CM}} \end{bmatrix} = -\begin{bmatrix} e^T\mathsf{R}_{qq}e & e^T\mathsf{R}_{qv} \\ \mathsf{R}_{vq}e & \mathsf{R}_{vv} \end{bmatrix}^{-1}\begin{bmatrix} e^T\mathsf{R}_{qq} \\ \mathsf{R}_{vq} \end{bmatrix} D^+\dot{x} \tag{34}$$

This is the first order ode that appears in (5).

REFERENCES

[1] D. P. Bertsekas and J. N. Tsitsiklis. *Neuro-dynamic programming*, volume 5. Athena Scientific Belmont, MA, 1996.

[2] J. Blair and T. Iwasaki. Optimal gaits for mechanical rectifier systems. *IEEE Trans. Automatic Control*, 56(1):59–71, 2011.

[3] S. Hirose. *Biologically inspired robots: snake-like locomotors and manipulators*. Oxford science publications. Oxford University Press, 1993.

[4] E. M Izhikevich. *Dynamical systems in neuroscience*. MIT press, 2007.

[5] P. G. Mehta and S. P. Meyn. Q-learning and pontryagin's minimum principle. In *Proceedings of the 48h IEEE Conference on Decision and Control (CDC) held jointly with 2009 28th Chinese Control Conference*, pages 3598–3605. IEEE, 2009.

[6] P. G. Mehta and S. P. Meyn. A feedback particle filter-based approach to optimal control with partial observations. In *52nd IEEE conference on decision and control*, pages 3121–3127. IEEE, 2013.

[7] E. Moulines and F. R. Bach. Non-asymptotic analysis of stochastic approximation algorithms for machine learning. In *Advances in Neural Information Processing Systems*, pages 451–459, 2011.

[8] M Saito, Masakazu Fukaya, and Tetsuya Iwasaki. Serpentine locomotion with robotic snakes. *IEEE Control Systems Magazine*, 22(1):64–81, 2002.

[9] C. Szepesvári. The asymptotic convergence-rate of q-learning. In *Advances in Neural Information Processing Systems*, pages 1064–1070, 1998.

[10] A. Taghvaei, S. A. Hutchinson, and P. G. Mehta. A coupled oscillators-based control architecture for locomotory gaits. In *Decision and Control (CDC), 2014 IEEE 53rd Annual Conference on*, pages 3487–3492. IEEE, 2014.

[11] A. K. Tilton, P. G. Mehta, and S. P. Meyn. Multi-dimensional feedback particle filter for coupled oscillators. In *2013 American Control Conference*, pages 2415–2421. IEEE, 2013.

[12] D. Vrabie, M. Abu-Khalaf, F. L. Lewis, and Y. Wang. Continuous-time adp for linear systems with partially unknown dynamics. In *2007 IEEE International Symposium on Approximate Dynamic Programming and Reinforcement Learning*, pages 247–253. IEEE, 2007.

[13] T. Wang, A. Taghvaei, and P. G. Mehta. Q-learning for POMDP: An application to locomotion gaits. In *58th IEEE Conference on Decision and Control (CDC)*. IEEE, 2019.